

VLBA determination of the distance to nearby star-forming regions

III. A preliminary distance to the Ophiuchus core with 4% accuracy

Laurent Loinard¹, Rosa M. Torres¹, Amy J. Mioduszewski² and Luis F. Rodríguez¹

ABSTRACT

The non-thermal 3.6 cm radio continuum emission from the young stars S1 and DoAr21 in the core of Ophiuchus, has been observed with the Very Long Baseline Array (VLBA) at 6 and 7 epochs, respectively, between June 2005 and August 2006. The typical separation between successive observations was 2 to 3 months. Thanks to the remarkably accurate astrometry delivered by the VLBA, the trajectory described by both stars on the plane of the sky could be traced very precisely, and modeled as the superposition of their trigonometric parallax and a uniform proper motion. The best fits yield distances to S1 and DoAr21 of $116.9_{-6.4}^{+7.2}$ and $121.9_{-5.3}^{+5.8}$, respectively. Combining these results, we estimate the mean distance to the Ophiuchus core to be $120.0_{-4.2}^{+4.5}$, a value consistent with several recent indirect determinations, but with a significantly improved accuracy of 4%. Both S1 and DoAr21 happen to be members of tight binary systems, but our observations are not frequent enough to properly derive the corresponding orbital parameters. This could be done with additional data, however, and would result in a significantly improved accuracy on the distance determination.

Subject headings: Astrometry — Stars: individual (S1, DoAr21) — Radiation mechanisms: non-thermal — Magnetic fields — stars: formation — Binaries: general

¹Centro de Radioastronomía y Astrofísica, Universidad Nacional Autónoma de México, Apartado Postal 72-3 (Xangari), 58089 Morelia, Michoacán, México; l.loinard@astrosmo.unam.mx

²National Radio Astronomy Observatory, Array Operations Center, 1003 Lopezville Road, Socorro, NM 87801, USA

1. Introduction

Ophiuchus is one of the most active regions of star-formation within a few hundred parsecs of the Sun (e.g. Lada & Lada 2003). It has played an important role in the development of our understanding of star-formation, and remains an important benchmark for this field of research. Indeed, it has been one of the key targets of the Spitzer c2d legacy program (Padgett et al. 2007); and has been observed in detail at numerous other wavelengths, including X-rays (Ozawa et al. 2005, Gagné et al. 2004), near-infrared (e.g. Haisch et al. 2002, Duchêne et al. 2004, and references therein), sub-millimeter (Motte et al. 1998, Johnstone et al. 2004), and radio (e.g. André et al. 1987, Leous et al. 1991).

The detailed analysis of this wealth of observational data has been somewhat hampered by the relatively large uncertainty on the distance to the Ophiuchus complex. Traditionally assumed to be at 165 pc (Chini 1981), it has recently been suggested to be somewhat closer. For example, de Geus et al. (1989) found a mean photometric distance of 125 ± 25 pc. Knude & Hog (1998), who examined the reddening of stars in the direction of Ophiuchus as a function of their Hipparcos distances, also found a clear extinction jump at 120 pc. Using a similar method, M. Lombardi et al. (in prep.) also find a distance of about 120 pc for the Ophiuchus core. Finally, Mamajek (2007) identified reflection nebulae within 5° of the center of Ophiuchus, and obtained the trigonometric parallax of the illuminating stars from the Hipparcos catalog. From the average of these Hipparcos parallaxes, he obtains a mean distance to Ophiuchus of 135 ± 8 pc.

This latter result is based on parallax measurements, but considers a fairly large area around Ophiuchus. It could, therefore, include objects unrelated to Ophiuchus itself. The former results are restricted to regions more concentrated on Ophiuchus, but they are based on indirect distance determinations. Here, we will present measurements of the trigonometric parallax of two young stars (S1 and DoAr21) directly associated with the Ophiuchus core. This will allow us to estimate directly the distance to this important region of star-formation.

2. Observed sources

The star S1 (of spectral type B4, $M \sim 6 M_\odot$) is among the brightest red and near-infrared objects in Ophiuchus (Grasdalen et al. 1973). It is also the brightest far-infrared member of the cluster (Fazio et al. 1976), a very bright X-ray source (ROX 14 –Montmerle et

al. 1983), and the brightest steady radio stellar object in Ophiuchus³ (Leous et al. 1991). S1 is fairly heavily obscured ($A_V \sim 10$), and there is clear evidence for an interaction between S1 and the dense gas associated with Oph A, and traced by DCO⁺ emission (Loren et al. 1990). Moreover, the age of the H II region excited by S1 is estimated to be about 5,000 yr (André et al. 1988). All this demonstrates that S1 can safely be assumed to be a member of the Ophiuchus core.

DoAr21 (Dolidze-Arakelyan 21) is a somewhat less massive star ($\sim 2.2 M_\odot$) of spectral type K1 (E. Jensen et al., in prep.). Like S1, it is fairly obscured ($A_V \sim 6\text{--}7$), and probably younger than 10^6 yr. It is associated with a bright X-ray source (ROX 8 –Montmerle et al. 1983), and with a strongly variable radio source (Feigelson & Montmerle 1985). Although it has long been classified as a naked T Tauri star (e.g. André et al. 1990), it was recently found to show a substantial infrared excess at $25 \mu\text{m}$ (Jensen et al. *ibid*) suggestive of a circumstellar disk. Given its youth, and location in the Ophiuchus core, DoAr21 is almost certainly also a *bona fide* member of the Ophiuchus complex.

As mentioned above, both S1 and DoAr21 are fairly strong radio sources. Indeed, both have been detected at 6 cm in previous Very Long Baseline Interferometry experiments: S1 with a flux density of 6–9 mJy (André et al. 1991), and DoAr21 with a flux density of nearly 10 mJy (Phillips et al. 1991).

3. Observations

In this paper, we will make use of two series of continuum 3.6 cm (8.42 GHz) observations obtained with the VLBA. Six observations of S1 were collected between June 2005 and August 2006, and seven observations of DoAr21 were obtained between September 2005 and August 2006 (See Tab. 1 for details). Each observation consisted of series of cycles with two minutes spent on source, and one minute spent on the phase-referencing quasar J1625–2527, located 1° south of both targets. J1625–2527 is a very compact extragalactic source whose absolute position ($\alpha_{J2000.0} = 16^{\text{h}}25^{\text{m}}46^{\text{s}}.8916, \delta_{J2000.0} = -25^\circ27'38''.327$) is known to better than 0.5 milli-arcsecond (mas –Beasley et al. 2002). The data were edited and calibrated using the Astronomical Image Processing System (AIPS –Greisen 2003). The basic data reduction followed the standard VLBA procedures for phase-referenced observations, and was described in detail in Loinard et al. (2007). Since the density of compact quasars known around Ophiuchus at the time of our observations was insufficient, we could not apply the

³DoAr21 –as shown by Feigelson & Montmerle (1985), and as we shall confirm below– can occasionally become brighter than S1.

multi-source calibration described in Torres et al. (2007).

Because of the significant overheads that were necessary to properly calibrate the data, only about 2 of the 4 hours of telescope time allocated to each of our observations were actually spent on source. Once calibrated, the visibilities were imaged with a pixel size of $50 \mu\text{as}$ after weights intermediate between natural and uniform ($\text{ROBUST} = 0$ in AIPS) were applied. This resulted in typical r.m.s. noise levels of 0.1 to 0.3 mJy depending on the weather conditions and source strength (Tab. 1). Both S1 and DoAr21 were detected with a signal to noise better than 7 at each epoch (Tab. 1).

4. Results, discussions and conclusions

4.1. Properties of S1

The mean 3.6 cm flux of S1 in our data is 4.8 mJy, and the dispersion about that mean is 1.2 mJy (see Fig. 1). This shows that S1 is variable at the level of about 25% on timescales of months to years. This modest level of variability is certainly not unexpected for a non-thermal source associated with an active stellar magnetosphere (Feigelson & Montmerle 1999). As mentioned earlier, André et al. (1991) reported a VLBI detection of S1 at 6 cm. They found –among many other things– that the source was somewhat resolved in their observations, with a full width at half maximum extension of about 1.7 mas. The radio emission associated with S1 is also found to be resolved in *all* six of our observations, with a deconvolved mean full width at half maximum of about 0.95 mas. This is somewhat smaller than the figure reported by André et al. (1991), but we note (i) that our observations and those of André et al. (1991) were obtained at different wavelengths; and (ii) that at some of our epochs, the size of the emission reached 1.5 mas, whereas at other epochs, it was smaller than 0.5 mas. At the distance of S1 (see below), 0.95 mas corresponds to about $24 R_{\odot}$. The diameter of S1 is expected to be about $8.5 R_{\odot}$ (André et al. 1991), so its magnetosphere appears to be on average 3 times more extended than its photosphere.

The fact that S1 is resolved, and that its size varies from epoch to epoch likely produces small random shifts in the photocenter of the radio emission with an amplitude of a fraction of the size of the emitting region. The true uncertainties on the position of S1 are, therefore, likely to be somewhat larger than the figures quoted in Tab. 1. Another factor that must be taken into account is that S1 is known to be a member of a binary system with a separation of about 20 mas (Richichi et al. 1994). The companion is inferred to be about 4 times dimmer than the primary at K band, so it is likely to be significantly less massive (Richichi et al. 1994). If we assume S1 to be a $6 M_{\odot}$ star (as suggested by its B4 spectral type), we

expect the orbital period to be about 0.7 yr, and the reflex motion of S1 to be about 1 to 2 mas if the companion is 10 to 20 times less massive than S1. Thus, the amplitude of the reflex motion is expected to be larger than the formal errors on the positions of S1 listed in Tab. 1.

4.2. Properties of DoAr21

The total radio flux of DoAr21 has long been known to be highly variable (Feigelson & Montmerle 1985). Our observations certainly confirm this strong variability since the ratio between the highest and the lowest measured flux exceeds 50 (Fig. 1). In particular, the flux during our first two observations (10–20 mJy) is systematically about an order of magnitude higher than that (0.4–2 mJy) at any of the following 5 observations. Unfortunately, our time coverage is too coarse to decide whether these first two epochs correspond to two different flares, or to a single long-duration one.

The extreme variability of DoAr21, while at odds with the situation in S1, is reminiscent of the case of the spectroscopic binary V773 Tau (e.g. Massi et al. 2002). In the latter source, Massi et al. (2002) showed that the variability had the same periodicity as the orbital motion, with the radio flux being highest at periastron. Interestingly, DoAr21 was found to be double during our second observation⁴. This suggests that the same mechanism that enhances the radio emission when the two binary components are nearest, might be at work in both objects. The separation between the two components of DoAr21 in our second observation is about 5 mas. This value, of course, corresponds to the projected separation; the actual distance between them must be somewhat larger. Moreover, if the mechanisms at work in DoAr21 and V773 Tau are similar, then DoAr21 must have been near periastron during our second epoch, and the orbit must be somewhat eccentric. As a consequence of these two effects, the semi-major axis of the orbit is likely to be a few times larger than the measured separation between the components at our second epoch, perhaps 10 to 15 mas. At the distance of DoAr21, this corresponds to 1.2 to 1.8 AU. For a mass of $2.2 M_{\odot}$ (see Sect. 1), the corresponding orbital period is 0.4 to 1.3 yr, and one would expect the source to oscillate with this kind of periodicity.

⁴The position given in Tab. 1 is that of the brightest of the two components. The other source is offset by more than 5 mas from its position of the steady component expected from the astrometry fits presented in §4.3.

4.3. Astrometry

The absolute positions of S1 and DoAr21 (listed in columns 3 and 4 of Tab. 1) were determined using a 2D Gaussian fitting procedure (task JMFIT in AIPS). This task provides an estimate of the position errors (also given in columns 3 and 4 of Tab. 1) based on the expected theoretical astrometric precision of an interferometer (Condon 1997). Systematic errors, however, usually limit the actual precision of VLBI astrometry to several times this theoretical value (e.g. Pradel et al. 2006, Loinard et al. 2007). Moreover, we have just seen that the extended magnetosphere of S1, and the reflex motions of both S1 and DoAr21 are likely to produce significant shifts in the positions of the source photocenters. While the effect of an extended magnetosphere might be to produce a random jitter, the reflex orbital motions ought to generate oscillations with a periodicity equal to that of the orbital motions. Our observations, however, are currently insufficient to properly fit full Keplerian orbits. Instead, in the present paper, we represent the possible systematic calibration errors as well as the jitter due to extended magnetospheres and the oscillations due to reflex motions, by a constant error term (the value of which will be determined below) that we add quadratically to the errors given in Tab. 1. The displacements of both S1 and DoAr21 on the celestial sphere are then modeled as a combination of their trigonometric parallaxes (π) and their proper motions (μ_α and μ_δ), assumed to be uniform and linear. The astrometric parameters were determined using a least-square fit based on a Singular Value Decomposition (SVD) scheme (see Loinard et al. 2007 for details). The reference epoch was taken at the mean of each set of observations (JD 2453757.63 \equiv J2006.061 for S1, and JD 2453796.52 \equiv J2006.167 for DoAr21). The best fit for S1 (Fig. 2a) yields the following astrometric parameters:

$$\begin{aligned} \alpha_{J2006.061} &= 16^{\text{h}}26^{\text{m}}34^{\text{s}}174127 \pm 0^{\text{s}}000026 \\ \delta_{J2006.061} &= -24^{\circ}23'28''44498 \pm 0''00028 \\ \mu_\alpha \cos \delta &= -3.88 \pm 0.87 \text{ mas yr}^{-1} \\ \mu_\delta &= -31.55 \pm 0.69 \text{ mas yr}^{-1} \\ \pi &= 8.55 \pm 0.50 \text{ mas.} \end{aligned}$$

For DoAr21, on the other and, we get (Fig. 2b):

$$\begin{aligned} \alpha_{J2006.167} &= 16^{\text{h}}26^{\text{m}}03^{\text{s}}018535 \pm 0^{\text{s}}000020 \\ \delta_{J2006.167} &= -24^{\circ}23'36''35830 \pm 0''00022 \\ \mu_\alpha \cos \delta &= -26.47 \pm 0.92 \text{ mas yr}^{-1} \end{aligned}$$

$$\begin{aligned}\mu_\delta &= -28.23 \pm 0.73 \text{ mas yr}^{-1} \\ \pi &= 8.20 \pm 0.37 \text{ mas.}\end{aligned}$$

To obtain a reduced χ^2 of 1 in both right ascension and declination, one must add quadratically 0.062 ms of time, and 0.67 mas to the statistical errors of S1 listed in Tab. 1, and 0.053 ms of time, and 0.57 mas to the statistical errors of DoAr21. These figures include all the unmodeled sources of positional shifts mentioned earlier. Interestingly, the residuals of the fit to the S1 data (inset in Fig. 2a) are not random, but seem to show a ~ 0.7 yr periodicity, as expected from the reflex motions (Sect. 4.1). Similarly, the residuals from the fit to DoAr21 seem to show a periodicity of ~ 1.2 yr (Fig. 2b, inset), within the range of expected orbital periods of that system (Sect. 4.2). This suggests that the errors are largely dominated by the unmodeled binarity of both sources, and that additional observations designed to provide a better characterization of the orbits ought to improve significantly the precision on the trigonometric parallax determinations.

The distance to S1 deduced from the parallax calculated above is $116.9_{-6.4}^{+7.2}$, while the distance deduced for DoAr21 is $121.9_{-5.3}^{+5.8}$. The weighted mean of these two parallaxes is 8.33 ± 0.30 , corresponding to a distance of $120.0_{-4.3}^{+4.5}$. Since both S1 and DoAr21 are *bone fide* members of the Ophiuchus core, this figure must represent a good estimate of the distance to this important region of star-formation. Note that it is in good agreement with several recent determinations (e.g. de Geus et al. 1989, Knude & Hog 1998, Lombardi et al. *ibid*), but with a significantly improved relative error of 4%. This level of accuracy is likely to be further improved once additional observations of S1 and DoAr21 designed to characterize their orbital motions are available. Such observations are currently being collected at the VLBA. A significant improvement in the distance estimate will also be obtained once the parallax to other sources (also currently observed at the VLBA) are measured.

L.L., R.M.T, and L.F.R. acknowledge the financial support of DGAPA, UNAM and CONACyT, México. NRAO is a facility of the National Science Foundation operated under cooperative agreement by Associated Universities, Inc.

REFERENCES

- Andre, P., Montmerle, T., & Feigelson, E. D. 1987, AJ, 93, 1182
 Andre, P., Montmerle, T., Feigelson, E. D., Stine, P. C., & Klein, K.-L. 1988, ApJ, 335, 940
 Andre, P., Montmerle, T., Feigelson, E. D., & Steppe, H. 1990, A&A, 240, 321

- Andre, P., Phillips, R. B., Lestrade, J.-F., & Klein, K.-L. 1991, *ApJ*, 376, 630
- Andre, P., Deeney, B. D., Phillips, R. B., & Lestrade, J.-F. 1992, *ApJ*, 401, 667
- Beasley, A. J., Gordon, D., Peck, A. B., Petrov, L., MacMillan, D. S., Fomalont, E. B., & Ma, C. 2002, *ApJS*, 141, 13
- Chini, R. 1981, *A&A*, 99, 346
- Condon, J. J. 1997, *PASP*, 109, 166
- Duchêne, G., Bouvier, J., Bontemps, S., André, P., & Motte, F. 2004, *A&A*, 427, 651
- Fazio, G. G., Low, F. J., Wright, E. L., & Zeilik, M., II 1976, *ApJ*, 206, L165
- Feigelson, E. D., & Montmerle, T. 1985, *ApJ*, 289, L19
- Feigelson, E.D., & Montmerle, T., 1999, *ARAA*, 37, 363
- Gagné, M., Skinner, S. L., & Daniel, K. J. 2004, *ApJ*, 613, 393
- de Geus, E. J., de Zeeuw, P. T., & Lub, J. 1989, *A&A*, 216, 44
- Grasdalen, G. L., Strom, K. M., & Strom, S. E. 1973, *ApJ*, 184, L53
- Greisen, E.W. 2003, in *Information Handling in Astronomy – Historical Vistas*, ed. A. Heck (Dordrecht: Kluwer Academic Publishers), 109
- Haisch, K. E., Jr., Barsony, M., Greene, T. P., & Ressler, M. E. 2002, *AJ*, 124, 2841
- Johnstone, D., Di Francesco, J., & Kirk, H. 2004, *ApJ*, 611, L45
- Knude, J., & Hog, E. 1998, *A&A*, 338, 897
- Lada, C. J., & Lada, E. A. 2003, *ARA&A*, 41, 57
- Leous, J. A., Feigelson, E. D., Andre, P., & Montmerle, T. 1991, *ApJ*, 379, 683
- Loinard, L., Torres, R. M., Mioduszewski, A. J., Rodríguez, L. F., González-Lópezlira, R. A., Lachaume, R., Vázquez, V., & González, E. 2007, *ApJ*, 671, 546
- Loren, R. B., Wootten, A., & Wilking, B. A. 1990, *ApJ*, 365, 269
- Mamajek, E. E. 2007, *ArXiv e-prints*, 709, arXiv:0709.0505
- Massi, M., Menten, K., & Neidhöfer, J. 2002, *A&A*, 382, 152

Montmerle, T., Koch-Miramond, L., Falgarone, E., & Grindlay, J. E. 1983, ApJ, 269, 182

Motte, F., Andre, P., & Neri, R. 1998, A&A, 336, 150

Ozawa, H., Grosso, N., & Montmerle, T. 2005, A&A, 438, 661

Padgett, D. L., et al. 2007, ArXiv e-prints, 709, arXiv:0709.3492

Pradel, N., Charlot, P., & Lestrade, J.-F. 2006, A&A, 452, 1099

Richichi, A., Leinert, C., Jameson, R., & Zinnecker, H. 1994, A&A, 287, 145

Torres, R. M., Loinard, L., Mioduszewski, A. J., & Rodríguez, L. F. 2007, ApJ, 671, 1813

Table 1: Observation results

Date	JD	α (J2000.0) $16^h 26^m$	δ (J2000.0) $-24^\circ 23'$	Flux (mJy)	Noise (mJy beam $^{-1}$)
S1					
2005 Jun 24	2453545.73	$34^s 1739533 \pm 0^s 0000015$	$28'' 426953 \pm 0'' 000056$	7.03 ± 0.56	0.28
2005 Sep 15	2453628.50	$34^s 1736922 \pm 0^s 0000020$	$28'' 432094 \pm 0'' 000062$	4.56 ± 0.47	0.23
2005 Dec 17	2453722.25	$34^s 1743677 \pm 0^s 0000012$	$28'' 441493 \pm 0'' 000044$	4.35 ± 0.35	0.19
2006 Mar 15	2453810.01	$34^s 1746578 \pm 0^s 0000019$	$28'' 451273 \pm 0'' 000048$	5.33 ± 0.41	0.17
2006 Jun 03	2453889.79	$34^s 1740172 \pm 0^s 0000006$	$28'' 455940 \pm 0'' 000023$	3.29 ± 0.13	0.07
2006 Aug 22	2453969.54	$34^s 1732962 \pm 0^s 0000012$	$28'' 462601 \pm 0'' 000050$	4.35 ± 0.22	0.09
DoAr21					
2005 Sep 08	2453621.52	$03^s 0189304 \pm 0^s 0000065$	$36'' 343394 \pm 0'' 00013$	11.78 ± 1.41	0.35
2005 Nov 16	2453691.33	$03^s 0191097 \pm 0^s 0000023$	$36'' 344504 \pm 0'' 00005$	20.34 ± 1.42	0.55
2006 Jan 08	2453744.19	$03^s 0191069 \pm 0^s 0000059$	$36'' 355803 \pm 0'' 00023$	0.39 ± 0.12	0.05
2006 Jan 19	2453755.16	$03^s 0191795 \pm 0^s 0000028$	$36'' 355677 \pm 0'' 00013$	0.97 ± 0.19	0.11
2006 Mar 28	2453822.97	$03^s 0189625 \pm 0^s 0000070$	$36'' 361924 \pm 0'' 00020$	1.49 ± 0.28	0.13
2006 Jun 04	2453890.78	$03^s 0182041 \pm 0^s 0000019$	$36'' 363763 \pm 0'' 00010$	1.92 ± 0.23	0.11
2006 Aug 24	2453971.53	$03^s 0169857 \pm 0^s 0000037$	$36'' 369957 \pm 0'' 00016$	1.45 ± 0.32	0.16

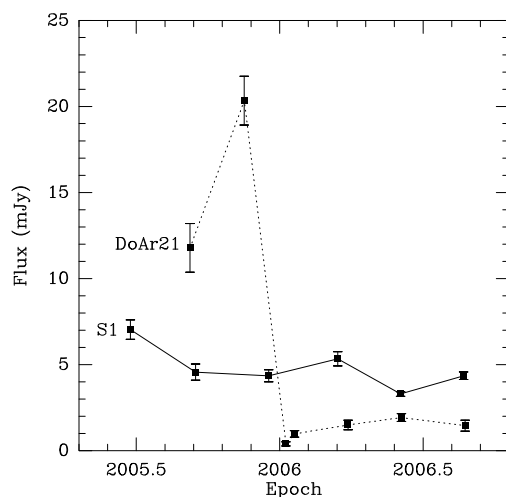


Fig. 1.— Radio flux of S1 (full line) and DoAr21 (dotted line) as a function of time.

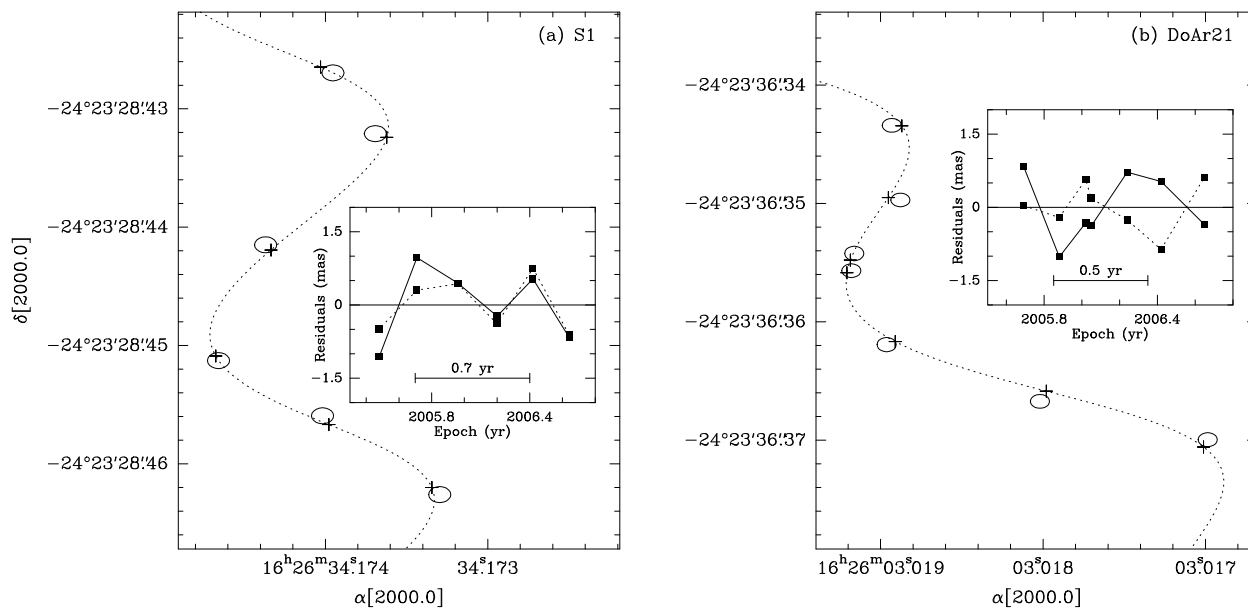


Fig. 2.— Measured positions and best fit for (a) S1, and (b) DoAr21. The observed positions are shown as ellipses, the size of which represents the magnitude of the errors. The positions at each epoch expected from the best fits are shown as + signs. The insets show the residuals (fit-observation) in right ascension (full line) and declination (dotted line).